Non-causal Linear Optimal Control of Wave Energy Converters with Enhanced Robustness by Sliding Mode Control

Yao Zhang, and Guang Li, *Member, IEEE*

***Abstract*—Sea wave energy converter control is a non-causal optimal control problem, and the control performance relies on the accuracy of wave prediction information. However, the existing wave prediction methods, such as Auto-Regressive (AR) method, extended Kalman Filter (EKF), Artificial neural network and deterministic sea wave prediction (DSWP), inevitably introduce prediction errors. This paper presents a robust non-causal linear optimal control of wave energy converters to explicitly cope with the prediction error of sea wave prediction and simultaneously compensate the modelling uncertainty caused by wave force approximations. This is achieved by designing a non-causal linear optimal control (LOC) to maximize the energy output and a sliding mode control (SMC) to compensate unmodeled WEC dynamics and wave prediction error. The parameters of both SMC and non-causal LOC are calculated off-line, which significantly enhances the real-time implementation of the proposed controller with reasonably low computational load. Simulation results demonstrate the efficacy of the proposed control strategy.**

***Index Terms*—Non-causal control, Sliding mode control, Wave Energy Converters, Prediction error, Modelling uncertainty**

I. Introduction

Sea waves provide an enormous source of renewable energy with high energy density and continuous power supply [1], [2]. To harness wave energy [3], many wave energy converters (WECs) have been developed, including oscillating water columns, overtopping WECs, point absorber and attenuators. It has also been recognized that WEC control is a non-causal control problem, which means the current control decision is based on the prediction of the incoming sea waves [4]. Recent studies show that wave prediction can play an important role in improving WEC control performance and maintaining safe operations compared to the counterpart of causal control, see [5]–[9].

Several prediction methods have been developed and applied to the WEC non-causal control problem. One class of prediction approaches are based on statistical methods, such as the Auto-Regressive (AR) prediction method [10] and the extended Kalman Filters (EKF) [11]. Artificial neural network (ANN) has also been used to forecast the short-term wave forces [12], [13]. Another class of prediction is based on the measurements of sea wave elevations at multiple upstream locations with certain distances away from the WEC, such as the deterministic sea wave prediction (DSWP) [14], which provides longer and more reliable wave prediction but at the cost of installation of extra more expensive hardware for wave measurements.

The accuracy of the prediction plays an important role in influencing WEC control performance. With inaccurate predictions of the wave excitation force or the wave elevation, the control performance can be degraded as shown in [15]–[17], where the sensitivity of non-causal control of WECs to prediction errors was fully analyzed. However, the prediction error has not been explicitly compensated for.

Sliding mode control (SMC) is a well-known nonlinear control strategy that has unique advantages in coping with robustness [18], [19], and has been widely applied in aerospace engineering [20], marine engineering [21] and permanent magnet synchronous motor system [22], etc. To maximize the energy output subject to prediction errors and modelling uncertainties, this paper proposes a SMC based non-causal linear optimal control (LOC) to maximize the energy output and simultaneously enhance the robustness by explicitly compensating the prediction error and the modelling uncertainty. The main novelties and contributions of the paper are summarized as follows:

- The wave prediction error and the modelling uncertainty are explicitly handled;
- Robust WEC control performance can be achieved with large prediction errors even in the absence of wave prediction;
- The proposed controller is computationally cheap so that it can be efficiently implemented in real-time;
- The tuning procedure is straightforward since the approach only has two tuning parameters.

Although the proposed controller can be applied to a wide variety of WEC devices, we select a particular WEC, called point absorber, as a case study for demonstration purpose. The schematic diagram of the point absorber is shown in Fig. 1. The proposed controller consists of a non-causal LOC and an additional term of SMC. The former is designed to maximize the energy output using the predicted wave information, and the latter is for coping with the prediction error and the modelling uncertainty.

The rest of the paper is as follows. Section II introduces a state-space model of the point absorber. The SMC based non-causal LOC is proposed in Section III, where the ability of compensating the prediction error and the modelling uncertainty is proven. Simulation results for the comparison

Y. Zhang is a postdoctoral researcher with Queen Mary University of London, UK, E1 4NS. e-mail: yao.zhang@qmul.ac.uk.

G. Li, the corresponding author, is with Queen Mary University of London, UK, E1 4NS. e-mail: g.li@qmul.ac.uk.

between the proposed controller and the non-causal LOC [5] are shown in Section IV. Section V concludes this paper.

II. State-space model of WEC

In this section, the dynamical model of a single-point-absorber is firstly introduced. To design the controller, the hydrodynamic model is transformed to a state-space model, which introduces modelling uncertainties.

A. Dynamical model of WEC

Fig. 1 shows part of a possible hydraulic power take-off (PTO) design: a hydraulic cylinder is vertically installed below the float and is fixed to the bottom of the seabed; more details on this design can be found in [23]. z_w and z_v are the water level and the height of the mid-point of the float respectively. The PTO torque is proportional to the force f_u acting on the piston inside the cylinder. The extracted power is $P := -f_u v$, where the velocity on the piston is $v := \dot{z}_v$.

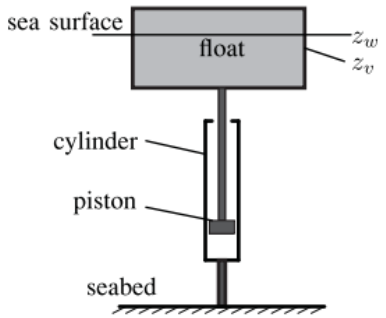

Fig. 1. Schematic diagram of the point absorber

By using Newton's second law, the dynamic equation [24] for the float of the point absorber is

$$m_s \ddot{z}_v = -f_s - f_r + f_e + f_u \tag{1}$$

where m_s is the float mass; the restoring force f_s is given by

$$f_s = k_s z_v \tag{2}$$

with the hydrostatic stiffness $k_s = \rho g s$, and ρ as water density, g as standard gravity, and s as the cross-sectional area of the float. f_r is the radiation force determined by

$$f_r = m_\infty \ddot{z}_v + \int_{-\infty}^{\infty} h_r(\tau)\dot{z}_v(t-\tau)d\tau \tag{3}$$

where m_∞ is the added mass; h_r is the kernel of the radiation force that can be computed via hydraulic software packages (e.g. WAMIT [25]). Following [24], the convolutional term in (3) $f_R := \int_{-\infty}^{\infty} h_r(\tau)\dot{z}_v(t-\tau)d\tau$ can be approximated by a causal finite dimensional state-space model

$$\dot{x}_r = A_r x_r + B_r \dot{z}_v \tag{4a}$$

$$f_R = C_r x_r \approx \int_{-\infty}^{t} h_r(\tau)\dot{z}_v(t-\tau)d\tau \tag{4b}$$

where (A_r, B_r C_r, 0) and $x_r \in \mathbb{R}^{n_r}$ are the state-space realisation and the state respectively. Following [24], the wave excitation force f_e can be determined by

$$f_e = \int_{-\infty}^{\infty} h_e(\tau) z_w(t-\tau)d\tau \tag{5}$$

where h_e is the kernel of the radiation force and the state-space approximation is given by

$$\dot{x}_e = A_e x_e + B_e z_w \tag{6a}$$

$$f_e = C_e x_e \approx \int_{-\infty}^{t} h_e(\tau) z_w(t-\tau)d\tau \tag{6b}$$

where (A_e, B_e C_e, 0) and $x_e \in \mathbb{R}^{n_e}$ are the state-space realization and the state respectively.

B. State-space model of a point-absorber

With the realizations of (4) and (6), the state-space model of (1) can be represented by

$$\begin{cases} \dot{x} = A_c x + B_{uc} u + B_{wc} w + \epsilon \\ y = C_c x \end{cases} \tag{7}$$

where $w := z_w$ is the wave elevation whose prediction is incorporated into the controller design, $y := z_v$, $y := \dot{z}_v$, $x := [z_v, \dot{z}_v, x_r, x_e]$, $u := f_u$. ϵ represents the modelling uncertainty caused by wave force approximations (4b) and (6b), and

$$\begin{aligned} A_c &= \begin{bmatrix} 0 & 1 & 0 & 0 \\ -\frac{k_s}{m} & 0 & \frac{C_e}{m} & -\frac{C_f}{m} \\ 0 & B_r & A_r & 0 \\ 0 & 0 & 0 & A_e \end{bmatrix} \quad B_{wc} = \begin{bmatrix} 0 \\ 0 \\ 0 \\ B_e \end{bmatrix} \quad B_{uc} = \begin{bmatrix} 0 \\ \frac{1}{m} \\ 0 \\ 0 \end{bmatrix} \\ C_c &= \begin{bmatrix} 0 & 1 & 0_{1\times(n_r+n_e)} \end{bmatrix} \end{aligned} \tag{8}$$

with $m := m_s + m_\infty$.

The continuous-time model (7) can be converted to a discrete time model

$$\begin{cases} x_{k+1} = A x_k + B_u u_k + B_w w_k + \epsilon_k \\ y_k = C x_k \end{cases} \tag{9}$$

where the pair (A, B_u, B_w, C) is the discrete-time form of the pair $(A_c, B_{uc}, B_{wc}, C_c)$.

III. non-causal Linear Optimal Control with Prediction Error Tolerance

In this section, the overall control strategy of the proposed controller is firstly introduced. The non-causal LOC and the SMC are then respectively designed, and the stability is proven. The computational load is also analyzed.

A. Control strategy

Define the prediction error of the wave elevation at each step as

$$\tilde{w} := w - \hat{w} \tag{10}$$

where $\hat{w}$ is the predicted wave elevation. The sequence of the prediction error is $\tilde{w}_{k,n_p} := [\tilde{w}_k, \tilde{w}_{k+1}, \ldots, \tilde{w}_{k+n_p-1}]$ with n_p the prediction step.

The optimal control problem for energy maximization is as follows:

$$\min_{u_0,\ldots,u_N} \Sigma_{k=0}^{N} \left\{ y_k u_k + \frac{1}{2} x_k^\top Q x_k + \frac{1}{2} R u_k^2 \right\} \tag{11}$$

subject to the perturbed state-space model (9).

The cost function consists of three terms. For the first term, since the power output is $P_k = -y_k u_k$, minimisation of $y_k u_k$ is equivalent to maximisation of power output. The second term represents the soft constraints on the state vector x_k. The weight Q is tuned to penalize some motions of the float. The third term aims to penalize the PTO torque by tuning the weight R. A good trade-off between these tuning weights needs to be determined to achieve the maximum energy output while not violating the constraints on the PTO limit and float motions for its safe operation. N is the number of time steps in the optimization process. In this case it is set to $N \to \infty$.

Differing from the non-causal controller proposed in [5], the solution of (11) is subject to a perturbed system with prediction errors, which leads to a challenge for maintaining optimality. To tackle this issue, a SMC is designed to eliminate the unknown modelling uncertainties and the prediction error in real-time and keep the actual dynamics of the system as a nominal one based on which the non-causal LOC is the optimal solution.

The state-space model (7) can be further written as

$$\dot{x} = A_c x + B_{uc} u + B_{wc} \hat{w} + B_{wc} \tilde{w} + \epsilon \tag{12}$$

The main idea of this paper is to design a SMC that fully eliminates the unknown terms $B_{wc}\tilde{w} + \epsilon$ and the prediction error $\tilde{w}_{k,n_p}$ so that the robustness is incorporated into the LOC. Owing to the attenuated uncertainty by SMC, the model dynamics approximates a nominal model (13) based on which the non-causal LOC generates the control law to maximize the energy output. Therefore, a prediction error tolerance control is achieved and the modelling uncertainty is compensated without losing the optimality of the non-causal LOC. The nominal model of (12) that ignores the unknown information is

$$\begin{cases} \dot{z} & = A_c z + B_c v + B_{wc} \hat{w} \\ y_z & = C_c z \end{cases} \tag{13}$$

where z is the nominal state and v is the nominal control input.

The discrete-time model of (13) is

$$\begin{cases} z_{k+1} & = A_k z_k + B_k v_k + B_{wk} \hat{w}_k \\ y_{zk} & = C_k z_k \end{cases} \tag{14}$$

The block diagram of the proposed controller is described in Fig. 2.

B. Controller design

Hypothesis 1. *Assume that the prediction error at each step $\tilde{w}$ and the modelling uncertainty ϵ are norm bounded, i.e. $\|\tilde{w}\| \le W$ and $\|\epsilon\| \le \varepsilon$ with $W \ge 0$ and $\varepsilon \ge 0$.*

The proposed controller is proposed as

$$u = u_{LOC} + u_{SMC} \tag{15}$$

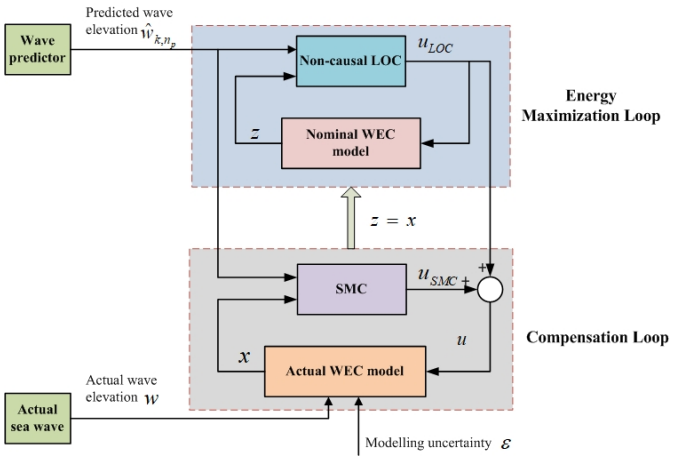

Fig. 2. Diagram of the proposed control strategy

The first term u_{LOC} is the non-causal LOC proposed in [5] depending on the predicted wave elevation $\hat{w}$. The second term u_{SMC} is determined by a sliding mode controller used to compensate the prediction error and the modelling uncertainty.

1) Design of u_{LOC}: It is reported in [5] that the solution of the following non-causal optimal problem without considering unknown uncertainties and prediction errors

$$\min_{u_0,\ldots,u_N} \Sigma_{k=0}^{N} \left\{ y_{zk} v_k + \frac{1}{2} z_k^\top Q z_k + \frac{1}{2} R v_k^2 \right\} \tag{16}$$

subject to the nominal state-space model (14) is in the form of

$$u_{LOC} = K_x z_k + K_d \hat{w}_{k,n_p} \tag{17}$$

with $\hat{w}_{k,n_p} := [\hat{w}_k, \hat{w}_{k+1}, \ldots, \hat{w}_{k+n_p-1}]$ being the predicted wave elevation and n_p being the length of wave prediction horizon.

The control input u_{LOC} consists of a feedback term with respect to the system states z_k and a feed-forward term with respect to the prediction of incoming wave elevation $\hat{w}_{k,n_p}$. K_x and K_d are constant coefficient matrices that can be pre-calculated off-line. The formulae for calculating them are

$$K_x = -(R + B_k^\top V B_k)^{-1}(C_k + B_k^\top V A_k) \tag{18}$$

$$K_d = -(R + B_k^\top V_{k+1} B_k)^{-1} B_k^\top \Psi \tag{19}$$

and

$$V = Q + A_k^\top V A_k - (C_k + B_k^\top V A_k)^\top (R + B_k^\top V B_k)^{-1}(C + B_k^\top V A_k) \tag{20}$$

where V is the solution of the algebraic Ricatti equation. Let $\Phi := (A_k + B_k K_x)^\top$, then Ψ in (19) is defined as $\Psi := [VB_{wk}, \Phi V B_{wk}, \ldots, \Phi^{n_p-1} V B_{wk}]$. Results in [5] show that with infinite control horizon $N \to \infty$ and finite wave prediction horizon n_p, the control law yields an unique solution.

2) Design of u_{SMC}: The second term of the input (15) is designed by

$$u_{SMC} = -\rho \text{sign}(\sigma) \tag{21}$$

where ρ is a constant satisfying $\rho \ge \delta$ with

$$\delta = \frac{\|GB_{wc}\|}{\|GB_{uc}\|} W + \frac{\|G\|}{\|GB_{uc}\|} \varepsilon + 2n_p \|K_d\| W \tag{22}$$

and the function $\text{sign}(\sigma)$ is defined as

$$\text{sign}(\sigma) = \begin{cases} \frac{\sigma}{\|\sigma\|}, & \sigma \neq 0 \\ 0, & \sigma = 0 \end{cases} \tag{23}$$

The sliding variable is designed as

$$\begin{aligned} \sigma =& G[x(t) - x(0) - \int_{t_0}^{t} (A_c x(\tau) \\ &+ B_{uc} u_{LOC} + B_{wc} \hat{w}(\tau) - n_p B_{uc} \|K_d\| W \text{sign}(\sigma)) d\tau] \end{aligned} \tag{24}$$

where G is such that GB_{uc} is invertible.

As shown in (22), the gain parameter of the sliding mode controller $u_{SMC} = -\rho \text{sign}(\sigma)$ is determined by three terms. The first two terms $\frac{\|GB_{wc}\|}{\|GB_{uc}\|} W + \frac{\|G\|}{\|GB_{uc}\|} \varepsilon$ are to cope with the inaccurate wave elevation at the current time and the modelling uncertainty caused by wave force approximations, respectively, and the last term $2n_p \|K_d\| W$ is to cope with the estimation error of the future wave elevation.

In the ideal situation where the non-causal LOC uses the accurate prediction, i.e. $u_{LOC} = K_x x_k + K_d w_{k,n_p}$. Applying the control policy (15) to the actual model (12), we have the actual state-space model as follows

$$\dot{x} = A_c x + B_{uc}(K_x x_k + K_d w_{k,n_p} - \rho \text{sign}(\sigma)) + B_{wc} w + \epsilon \tag{25}$$

The nominal model (13) that is not aware of modelling uncertainties and prediction errors is as follows

$$\dot{z} = A_c z + B_{uc}(K_x z_k + K_d \hat{w}_{k,n_p}) + B_{wc} \hat{w} \tag{26}$$

Since the prediction error and the modelling uncertainty are both unknown, we aim to prove that by using the control policy (15), the actual ideal model (25) that contains unknown information can be approximated by the nominal model (26) that uses available information. Therefore, owing to the compensation by SMC, the control performance can be maintained by using available but inaccurate information.

Theorem 1. *By using the sliding mode controller* (21)*, the prediction error and the modelling uncertainty can be eliminated and the closed-loop dynamics of* (25) *approximates the nominal model* (26)*.*

Proof. Step 1: to prove that the proposed sliding mode $\sigma = \dot{\sigma} = 0$ can be maintained.

Select a Lyapunov candidate as $V = 0.5\sigma^2$, and its time derivative is

$$\begin{aligned} \dot{V} =& \sigma \dot{\sigma} \\ =& G\sigma(\dot{x} - A_c x - B_{uc} u_{LOC} - B_{wc} \hat{w} \\ &+ n_p B_{uc} \|K_d\| W \text{sign}(\sigma)) \\ =& G\sigma(-B_{uc} \rho \text{sign}(\sigma) + B_{wc} \tilde{w} + \epsilon + \\ &+ n_p B_{uc} \|K_d\| W \text{sign}(\sigma) + B_{uc} K_d \tilde{w}_{k,n_p}) \\ \leq& - \|\sigma\|(\|GB_{uc}\|\rho - (\|GB_{wc}\|\|\tilde{w}\| + \|G\|\|\epsilon\| \\ &+ 2n_p \|GB_{uc}\|\|K_d\|W)) \\ \leq& - \|\sigma\|(\|GB_{uc}\|\rho - (\|GB_{wc}\|W + \|G\|\varepsilon \\ &+ 2n_p \|GB_{uc}\|\|K_d\|W)) \end{aligned} \tag{27}$$

Since $\rho \geq \delta$ with $\delta = \frac{\|GB_{wc}\|}{\|GB_{uc}\|} W + \frac{\|G\|}{\|GB_{uc}\|} \varepsilon + 2n_p \|K_d\| W$, we have $\dot{V} \leq 0$. Therefore, the $\sigma = \dot{\sigma} = 0$ can be maintained.

Step 2: to prove that once the sliding mode is maintained, the closed-loop dynamics becomes the nominal model.

If $\sigma = \dot{\sigma} = 0$ holds, then we have

$$\dot{\sigma} = G(\dot{x} - A_c x - B_{uc} u_{LOC} - B_{wc} \hat{w}) = 0 \tag{28}$$

which yields

$$\dot{x} = A_c x + B_{uc} u_{LOC} + B_{wc} \hat{w} \tag{29}$$

Combining (13) and (29) and applying the nominal input as $v = u_{LOC}$, the closed-loop state in the sliding mode approximates the nominal state, i.e. $z = x$. This completes the proof. □

From Theorem 1, by applying the proposed SMC (21), we have $z_k = x_k$. Therefore, the solution of the non-causal optimal problem (11) is (15) with

$$u_{LOC} = K_x x_k + K_d \hat{w}_{k,n_p} \tag{30}$$

C. Controller Analysis

The proposed controller achieves the prediction-error-tolerance and modelling-uncertainty-tolerance control by designing a SMC to compensate the unknown prediction error and the unknown modelling uncertainty. This controller is computationally econmic so that it is applicable in practice due to the following reasons:

- For the term of non-causal LOC, the gain parameters K_x and K_d are determined off-line with a specific pair of the weighting matrix (Q, R);
- For the additional term of the SMC, it only has one parameter ρ, which technically satisfies $\rho \geq \delta$ as stated in Theorem 1. For further simplicity, this parameter can be chosen as $\rho = \delta$ in practice leading to no parameters needed to be tuned.

IV. Simulation Results

Simulation is run by Matlab/Simulink 2017b. The sampling rate is 0.1 s. The parameters of the WEC model summarized in Table I and the hydrodynamic coefficients are adopted from those used in [24] and [5] for comparison purpose.

TABLE I
THE PARAMETERS USED FOR THE WEC MODEL

Description	Notation	values
Stiffness	k_s	3866 N/m
Float mass	m_s	242 kg
Added mass	m_∞	83.5 kg
Total mass	m	325.5 kg
Device width	DW	0.7 m
Input force limit	$u_{\max}$	8 kN
Float heave limit	$\Phi_{\max}$	0.5 m

The state-space matrices of the impulse function for calculating the wave excitation force [5], [24] is

$$A_e = \begin{bmatrix} 0 & 0 & 0 & 0 & -400 \\ 1 & 0 & 0 & 0 & -459 \\ 0 & 1 & 0 & 0 & -226 \\ 0 & 0 & 1 & 0 & -64 \\ 0 & 0 & 0 & 1 & -9.96 \end{bmatrix}, B_e = \begin{bmatrix} 1549886 \\ -116380 \\ 24748 \\ -644 \\ 19.3 \end{bmatrix},$$

$$C_e = \begin{bmatrix} 0 & 0 & 0 & 0 & 1 \end{bmatrix}$$

The state-space matrices of the impulse function for calculating the radiation force [5], [24] is

$$A_r = \begin{bmatrix} 0 & 0 & -17.9 \\ 1 & 0 & -17.7 \\ 0 & 1 & -4.41 \end{bmatrix}, B_r = \begin{bmatrix} 36.5 \\ 394 \\ 75.1 \end{bmatrix},$$
$$C_r = \begin{bmatrix} 0 & 0 & 1 \end{bmatrix}$$

which result in a WEC state-space model with an order of 10.

A realistic sea wave heave trajectory gathered from the coast of Cornwall, UK, is properly scaled by Froude scaling according to the size of the point absorber. As shown in Fig. 3 and reported in [5], for the point absorber with parameters in Table I, the energy output increases significantly when the wave prediction horizon is within 3 s, and the WEC non-causal LOC with longer wave prediction has a better performance; however, the benefit of further increasing wave prediction horizon over 3 s becomes less obvious.

Therefore, we choose the prediction horizon as 3 s in the sequel to present the best control performance of non-causal LOC.

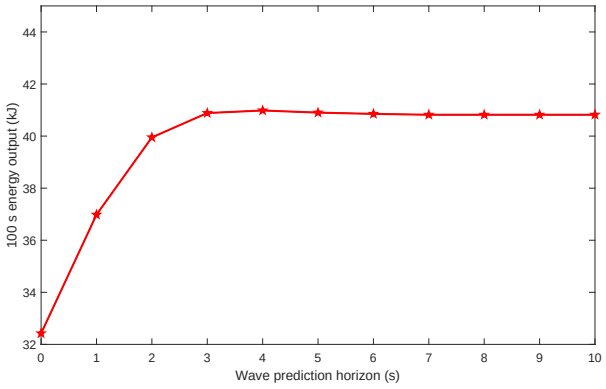

Fig. 3. Wave elevation used in simulation and energy output with different wave predictions

Two sets of simulation are done to verify the effectiveness and robustness of the proposed SMC based LOC. For comparison purpose, the control performance of both the proposed SMC based non-causal LOC (15) and the non-causal LOC (17) proposed in [5] is tested. Both of the two controllers share the same choice of the weighting matrixes: $Q = \text{diag}\{6, 9.8, 0, ..., 0\}$ and $R = 0.08$ [5].

Simulation A: The unknown modelling uncertainty is firstly ignored, i.e. $\epsilon = 0$, and the prediction error of the future wave elevation is considered. The energy outputs of both the proposed SMC based non-causal LOC (15) and the non-causal LOC (17) proposed in [5] are demonstrated in the simulation.

Simulation B: By taking both the prediction error of the future wave elevation and the unknown modelling uncertainty acting on the WEC ϵ into consideration, the proposed SMC based non-causal LOC is verified to be effective to cope with the modelling uncertainty and prediction errors simultaneously. Two uncertain models (i.e. models with uncertainties) are considered in Simulation B. In the uncertain model (a), the parametric uncertainty is considered. In the uncertain model (b), the nonlinear effects of the linear wave force such as Froude Krylov (FK) forces is taken into account.

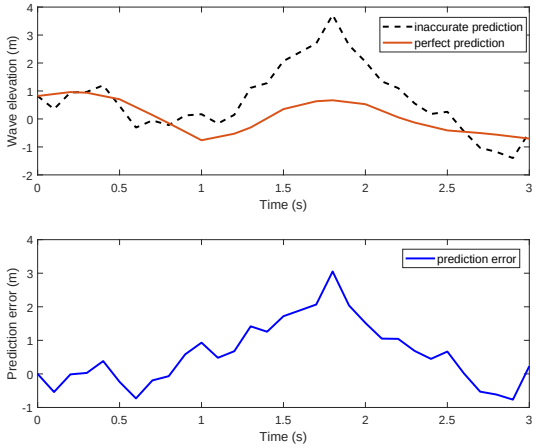

Fig. 4. Inaccurate 3s prediction of the future wave elevation

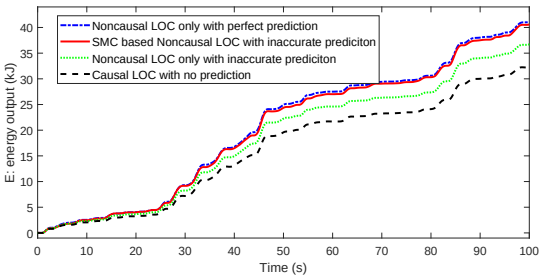

Fig. 5. Energy output of LOC and SMC based LOC with perfect and inaccurate predictions

A. Control performance with prediction error and no modelling uncertainty

In this subsection, the unknown model uncertainty is not considered, i.e. $\epsilon = 0$. The prediction error is modelled in the following form

$$\tilde{w}(k+1) = \lambda \tilde{w}(k) + \xi_k, k = 1, ..., N \tag{31}$$

where $N > 0$ is the prediction step, $\lambda = 1.0001$ is taken, making the filter unstable, to match with realistic prediction errors that grows with the prediction time. Both $\xi_k \sim \mathcal{N}(0, 0.1)$ and $\tilde{w}_0 \sim \mathcal{N}(0, 0.8)$ are Gaussian white noises. With the prediction error shown in Fig. 4 as an example, the control performance of both LOC and SMC based LOC is demonstrated in Figs. 5 $\sim$ 6.

From Figs. 5 and 6, it can be found from the comparison between the causal LOC (the black dashed line) and the non-causal LOC with perfect prediction (the blue dotted line) that the energy output significantly increases by 36.8%. While with an inaccurate prediction shown in Fig. 4, the control performance of the non-causal LOC (the green dotted line) is degraded with 16.4% energy loss compared with the control performance of the non-causal LOC with perfect prediction

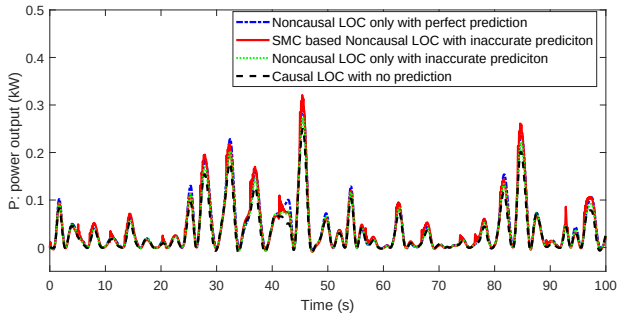

Fig. 6. Power output of LOC and SMC based LOC with perfect predictions and without predictions

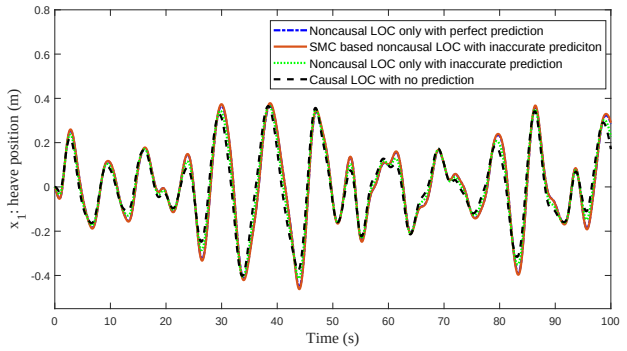

Fig. 7. Heave position of the float of LOC and SMC based LOC with perfect and inaccurate predictions

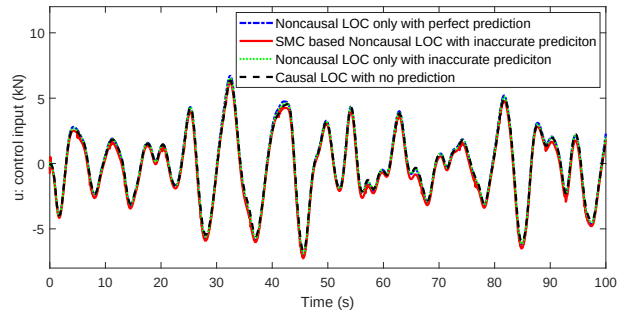

Fig. 8. Control input of LOC and SMC based LOC with perfect predictions and without predictions

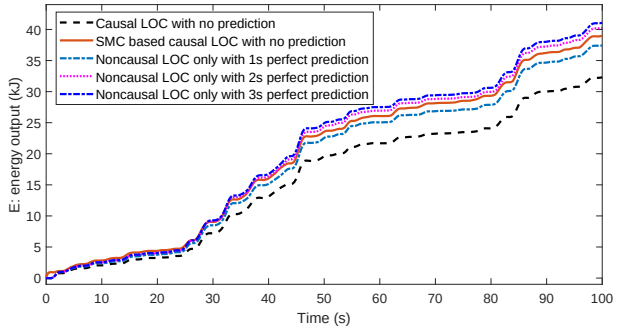

Fig. 9. Energy output of LOC and SMC based LOC with different prediction horizons

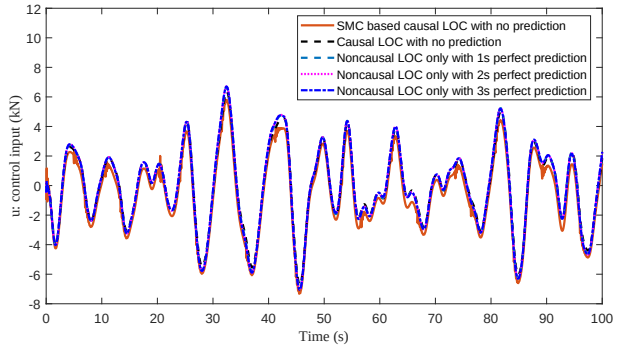

Fig. 10. Control input of LOC and SMC based LOC with different prediction horizons

(the blue dotted line). By using the proposed SMC based non-causal LOC (the red line), the control performance is barely affected by the prediction error with only 1.8% energy loss. This verifies the effectiveness of the proposed SMC based non-causal LOC on coping with the prediction error.

From Figs. 7, it can be seen that the float heave trajectories are all within the limit, which ensure safe operations. By comparing the control input of the SMC based non-causal LOC with other control inputs in Fig. 8, we can see that the magnitude of the control input signal does not significantly change when the sliding mode term is added, which means no extra PTO torque limit is required.

To further verify the robustness of the proposed SMC based approach for causal LOC, prediction is assumed completely unknown for SMC to compensate the 100 % prediction error. Figs. 9 and 10 show that compared with the non-causal LOC with 1 s prediction and 2 s prediction, the proposed SMC based non-causal LOC can ensure an acceptable energy output without using any predictions, and the maximal magnitudes of the control input are similar. The energy output of the causal SMC based LOC is between that of non-causal LOC with 1s prediction and that of non-causal LOC with 2s prediction, which increases 26.8% compared with that of the causal LOC (the black dashed line). This verifies the ability of the proposed controller to compensate the future wave prediction errors by treating them as completely unknown disturbances. Therefore, the proposed controller can be used to recover control performance of non-causal controller to a large extent in the absence of prediction.

In order to compare the control performance in different sea environments, simulations of different wave profiles (defined by significant wave height H_s and wave peak period T_p) are run. Capture width ratio (CWR) is calculated to demonstrate the energy conversion capability, which is $CWR = P_{av}/DW/P_w$ [26] where P_{av} is the average mechanical power, P_w is wave power per meter width of wave crest (integrated from spectra), and DW is the device width. For the point absorber with parameters shown in Table I, the device width is $DW = 0.7$ m.

Fig. 11 shows the CWR of the point absorber obtained from a wide range of simulations under JONSWAP (Joint

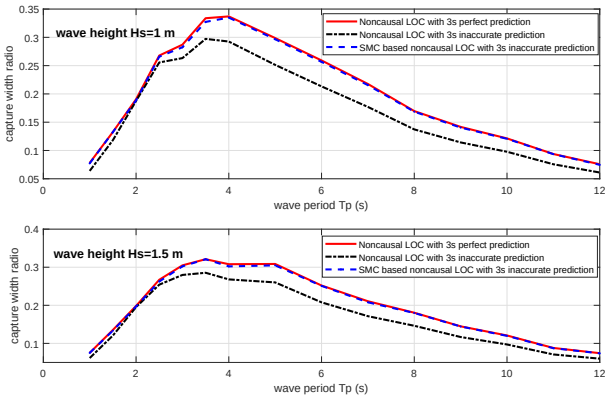

Fig. 11. Capture width ratio with perfect and inaccurate predictions ($H_s = 1$ m and $H_s = 1.5$ m)

North Sea Wave Project) wave model with spectral peakedness factor of unity to generate irregular wave spectra and the significant wave heights are $H_s = 1$ m and $H_s = 1.5$ m. Wave peak period ranges from 1s to 12s with 1s interval. The control performance of the proposed SMC based non-causal LOC barely affected by the prediction error in different sea environments.

B. Control performance with prediction error and modelling uncertainty

In this subsection, both the prediction error and the modelling uncertainty are considered. The robustness of the proposed controller subject to modelling mismatch and prediction error is verified.

To verify the efficacy of SMC to cope with parametric uncertainties and wave forces error, two forms of uncertainties are considered in the model respectively as :

- **Uncertain model (a)**: the added mass used in the control is 18.4 kg which is 78% less than the nominal value of WEC added mass. Thus the total mass used in the control design is $242 + 18.4 = 260.4$ kg, which is 20% less than the nominal value of WEC total mass. The controllers are designed based on the nominal model, and the plant is the perturbed model.
- **Uncertain model (b)**: to introduce the static FK force to the model, the coefficient of restoring force (2) in the control design is changed from 3866 N/m to $3866 \times 1.5 = 5799$ N/m; to introduce the dynamic FK force to the model, the coefficient of the excitation force C_e (6b) in the controller design is changed from $C_e = \begin{bmatrix} 0 & 0 & 0 & 0 & 1 \end{bmatrix}$ to $C_e = \begin{bmatrix} 0 & 0 & 0 & 0 & 1 + 0.5 r_s(k) \end{bmatrix}$ with $r_s(k) \in (0, 1)$ being a random series, $k = 1...N$. The resulting model deviation is equivalent to a model uncertainty that is greater than 40% of the nominal model, which is sufficiently large for verifying the effectiveness of SMC in coping with the nonlinear effect.

The controllers are designed based on the nominal model, and the plant is based on the uncertain model.

With the modelling uncertainties described in (a) and 3 s of wave predictions, the energy output of the non-causal LOC and the proposed SMC based non-causal LOC is shown in Fig. 12, from which we have the following findings.

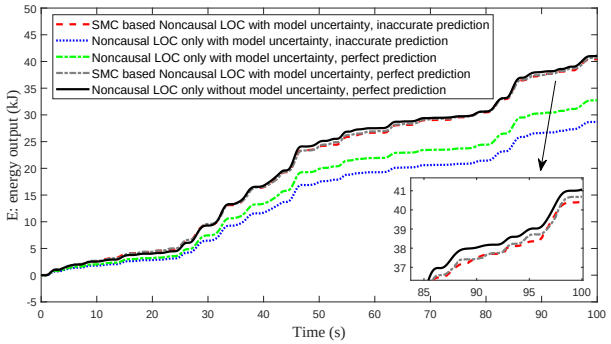

Fig. 12. Energy output of accurate and uncertain model (a) with perfect and inaccurate predictions

Firstly, we consider the case of 3 s perfect prediction. Compared with the non-causal LOC without any modelling uncertainties, i.e. $\epsilon = 0$ (the black line), the control performance of the non-causal LOC is degraded with 27.1% energy loss compared to the case when the modelling uncertainties are taken into account (the green dotted line). However, the control performance of the proposed SMC based non-causal LOC (the grey dotted line) is barely affected with only 1.03% energy loss subject to the modelling uncertainty. Therefore, the proposed SMC based non-causal LOC can cope with the unknown modelling uncertainty and maintain the energy maximization.

Secondly, we consider the case of 3 s inaccurate prediction shown in Fig. 4. The non-causal LOC generates further less energy (the blue dotted line) in the situation where both the modelling uncertainty and the prediction error are added than the non-causal LOC without modelling uncertainty and prediction error (the black line). However, compared with the energy output of the non-causal LOC without modelling uncertainties and no prediction error (the black line), the one of the proposed SMC based non-causal LOC subject to both modelling uncertainty and prediction error (the red dashed line) barely decreases with only 1.25% energy loss. Therefore, the proposed SMC based non-causal LOC can cope with the unknown modelling uncertainty and the prediction error simultaneously.

Fig. 13 shows that the heave position trajectories of the float are all within heave limitations, therefore, safe operations are ensured. The corresponding control inputs are shown in Fig. 14, from which we can find that the magnitude of a maximal control input signal does not significantly change when the sliding mode term is added leading to a fair comparison basis between the non-causal LOC and the proposed SMC based non-causal LOC.

Fig. 15 shows the CWR of the point absorber obtained from a wide range of simulations under JONSWAP wave model with spectral peakedness factor of unity to generate irregular wave spectra and the significant wave heights are $H_s = 1$ m and $H_s = 1.5$ m. Wave peak period ranges from 1s to 12s with 1s interval. The modelling uncertainty and the prediction

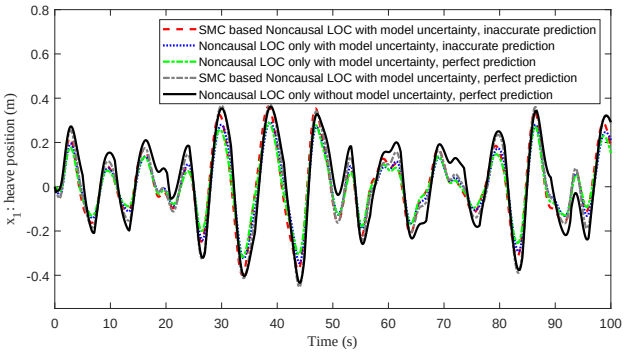

Fig. 13. Heave position of the float of accurate and uncertain model (a) with perfect and inaccurate predictions

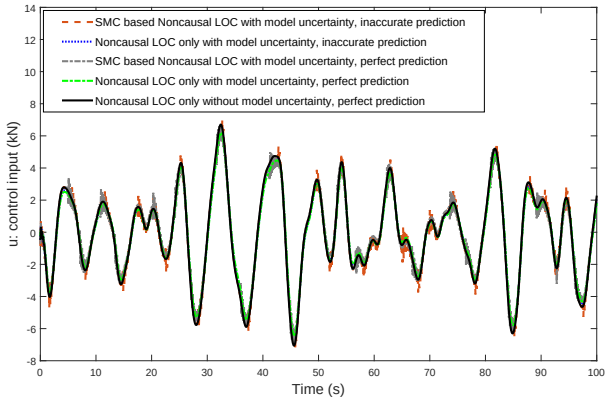

Fig. 14. Control input of accurate and uncertain model (a) with perfect and inaccurate predictions

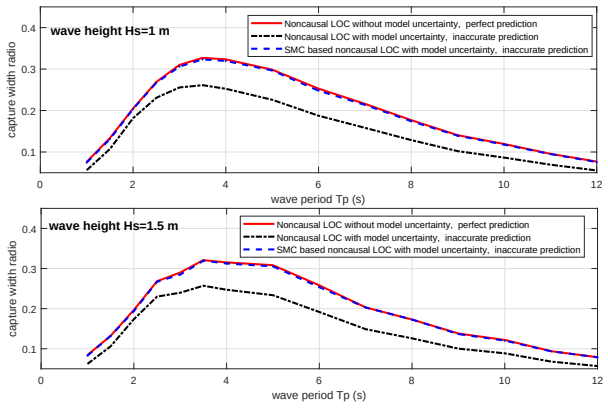

Fig. 15. Capture width ratio with uncertain model (a) and inaccurate predictions ($H_s = 1$ m and $H_s = 1.5$ m)

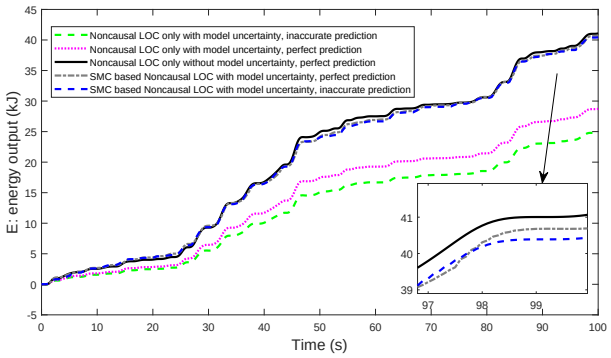

Fig. 16. Energy output of accurate and uncertain model (b) with perfect and inaccurate predictions

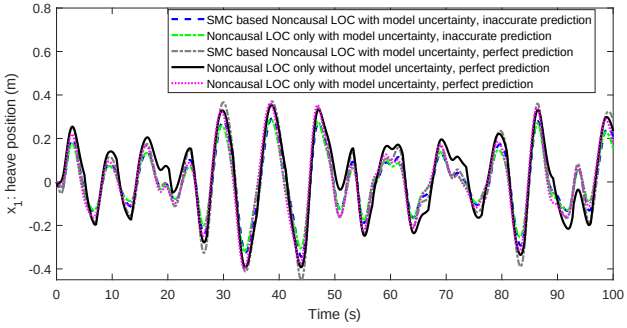

Fig. 17. Heave position of the float of accurate and uncertain model (b) with perfect and inaccurate predictions

error are both considered. It can be found that the proposed SMC based non-causal LOC can cope with the prediction error and the modelling uncertainty simultaneously in different sea environments.

In order to further verify the effectiveness of the proposed method in handling the nonlinear effects in linear forces such as the FK force, we consider the uncertain model (b) which introduces more than 40% model uncertainty to the model. With the modelling uncertainties described in (b) and 3 s of wave predictions, the simulation results of the non-causal LOC and the proposed SMC based non-causal LOC are shown in Figs. 16 $\sim$ 19.

It can be found from Figs. 12 and 16 that for the non-causal LOC, the control performance with the uncertain model (b) (the green dashed line in Fig. 16) is further degraded by 13.51% energy loss by comparison with the one with the uncertain model (a) (the blue dotted line in Fig. 12), which means a more significant model uncertainty is added to the model. While for the proposed SMC based non-causal LOC, the control performance (the blue dashed line in Fig. 16) is barely degraded by only 0.7% energy loss by comparison with the one with the uncertain model (a) (the red dashed line in Fig. 12). This further verifies the robustness against the nonlinear effects of the proposed method. Therefore, the proposed method is quite robust to deal with the uncertainty and the prediction error.

Fig. 17 shows that the heave position trajectories of the

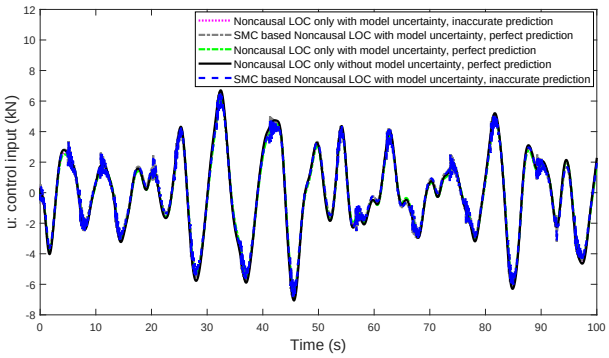

Fig. 18. Control input of accurate and uncertain model (b) with perfect and inaccurate predictions

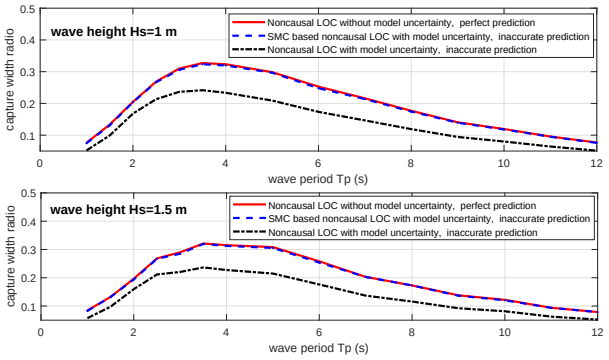

Fig. 19. Capture width ratio with uncertain model (b) and inaccurate predictions ($H_s = 1$ m and $H_s = 1.5$ m)

float are all within heave limitations, therefore, safe operations are ensured by the proposed controller. The corresponding control inputs are shown in Fig. 18, from which we can find that the magnitude of a maximal control input signal does not significantly change when the sliding mode term is added leading to a fair comparison basis between the non-causal LOC and the proposed SMC based non-causal LOC.

Fig. 19 shows the CWR of the point absorber obtained from a wide range of simulations under JONSWAP wave model with spectral peakedness factor of unity to generate irregular wave spectra and the significant wave heights are $H_s = 1$ m and $H_s = 1.5$ m. Wave peak period ranges from 1s to 12s with 1s interval. It can be found that the proposed SMC based non-causal LOC can cope with the prediction error and the modelling uncertainty described in the uncertain model (b) simultaneously in different sea environments.

V. Conclusions

A novel SMC based non-causal LOC has been proposed in this paper to explicitly cope with the prediction error of the future wave elevation and also the unknown modelling uncertainties. The robust stability subject to the unknown prediction errors and uncertainties has been proven. Since the parameters of the proposed controller are determined off-line, the computational amount is low enough for the control approach to be efficiently implemented on economically viable computational hardware. Future work is applying the proposed control scheme to the multi-mode WEC control system.

Acknowledgement

This work was supported in part by a research contract from Wave Energy Scotlands Control Systems programme, in part by EPSRC grant Launch and Recovery in Enhanced Sea States (no. EP/P023002/1) and in part by Newton Advanced Fellowship (NA160436) by Royal Society.

References

[1] Alain Clément, Pat McCullen, António Falcão, Antonio Fiorentino, Fred Gardner, Karin Hammarlund, George Lemonis, Tony Lewis, Kim Nielsen, Simona Petroncini, et al. Wave energy in europe: current status and perspectives. *Renewable and sustainable energy reviews*, 6(5):405–431, 2002.

[2] Raul Banos, Francisco Manzano-Agugliaro, FG Montoya, Consolacion Gil, Alfredo Alcayde, and Julio Gómez. Optimization methods applied to renewable and sustainable energy: A review. *Renewable and sustainable energy reviews*, 15(4):1753–1766, 2011.

[3] Benjamin Drew, Andrew R Plummer, and M Necip Sahinkaya. A review of wave energy converter technology, 2009.

[4] Johannes Falnes. *Ocean waves and oscillating systems: linear interactions including wave-energy extraction*. Cambridge university press, 2002.

[5] Siyuan Zhan and Guang Li. Linear optimal noncausal control of wave energy converters. *IEEE Transactions on Control Systems Technology*, 2018.

[6] Guang Li and Michael R Belmont. Model predictive control of sea wave energy converters–part i: A convex approach for the case of a single device. *Renewable Energy*, 69:453–463, 2014.

[7] Jørgen Hals, Johannes Falnes, and Torgeir Moan. Constrained optimal control of a heaving buoy wave-energy converter. *Journal of Offshore Mechanics and Arctic Engineering*, 133(1):011401, 2011.

[8] Romain Genest and John V Ringwood. A critical comparison of model-predictive and pseudospectral control for wave energy devices. *Journal of Ocean Engineering and Marine Energy*, 2(4):485–499, 2016.

[9] John V Ringwood, Giorgio Bacelli, and Francesco Fusco. Energy-maximizing control of wave-energy converters: The development of control system technology to optimize their operation. *IEEE Control Systems Magazine*, 34(5):30–55, 2014.

[10] Yao Zhang, Tianyi Zeng, and Guang Li. Robust excitation force estimation and prediction for wave energy converter m4 based on adaptive sliding-mode observer. *IEEE Transactions on Industrial Informatics*, 2019.

[11] Francesco Fusco and John V Ringwood. Short-term wave forecasting for real-time control of wave energy converters. *IEEE Transactions on sustainable energy*, 1(2):99–106, 2010.

[12] Liang Li, Zhiming Yuan, and Yan Gao. Maximization of energy absorption for a wave energy converter using the deep machine learning. *Energy*, 165:340–349, 2018.

[13] Liang Li, Zhen Gao, and Zhi-Ming Yuan. On the sensitivity and uncertainty of wave energy conversion with an artificial neural-network-based controller. *Ocean Engineering*, 183:282–293, 2019.

[14] L Abusedra and MR Belmont. Prediction diagrams for deterministic sea wave prediction and the introduction of the data extension prediction method. *International Shipbuilding Progress*, 58(1):59–81, 2011.

[15] Francesco Fusco and John Ringwood. A model for the sensitivity of non-causal control of wave energy converters to wave excitation force prediction errors. In *Proceedings of the 9th European Wave and Tidal Energy Conference (EWTEC)*. School of Civil Engineering and the Environment, University of Southampton, 2011.

[16] Liang Li, Zhiming Yuan, Yan Gao, and Xinshu Zhang. Wave force prediction effect on the energy absorption of a wave energy converter with real-time control. *IEEE Transactions on Sustainable Energy*, 10(2):615–624, 2018.

[17] Xiantao Zhang, Jianmin Yang, Wenhua Zhao, and Longfei Xiao. Effects of wave excitation force prediction deviations on the discrete control performance of an oscillating wave energy converter. *Ships and Offshore Structures*, 11(4):351–368, 2016.

[18] Christopher Edwards and Sarah Spurgeon. *Sliding mode control: theory and applications*. Crc Press, 1998.

[19] Yao Zhang, Guangfu Ma, Yanning Guo, and Tianyi Zeng. A multi power reaching law of sliding mode control design and analysis. *Acta Automatica Sinica*, 42(3):466–472, 2016.
[20] Yao Zhang, Ranjan Vepa, Guang Li, and Tianyi Zeng. Mars powered descent phase guidance design based on fixed-time stabilization technique. *IEEE Transactions on Aerospace and Electronic Systems*, 2018.
[21] Jun-Jie Ren, Yan-Cheng Liu, Ning Wang, and Si-Yuan Liu. Sensorless control of ship propulsion interior permanent magnet synchronous motor based on a new sliding mode observer. *ISA transactions*, 54:15–26, 2015.
[22] Hongryel Kim, Jubum Son, Jangmyung Lee, et al. A high-speed sliding-mode observer for the sensorless speed control of a pmsm. *IEEE Transactions on Industrial Electronics*, 58(9):4069–4077, 2011.
[23] G Weiss, G Li, M Mueller, S Townley, and MR Belmont. Optimal control of wave energy converters using deterministic sea wave prediction. *Fuelling the Future: Advances in Science and Technologies for Energy Generation, Transmission and Storage*, page 396, 2012.
[24] Z Yu and J Falnes. State-space modelling of a vertical cylinder in heave. *Applied Ocean Research*, 17(5):265–275, 1995.
[25] Chang-Ho Lee. *WAMIT theory manual*. Massachusetts Institute of Technology, Department of Ocean Engineering, 1995.
[26] A Babarit. A database of capture width ratio of wave energy converters. *Renewable Energy*, 80:610–628, 2015.

Yao Zhang received her Ph. D. in Department of Control Science and Engineering, specialized in control systems and deep space explorations, from Harbin Institute of Technology, in 2018. She is currently a postdoctoral researcher in Queen Mary University of London. Her research interest covers sliding mode control, model predictive control and control applications, etc.

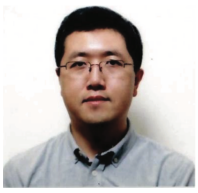

Guang Li (M'09) received his Ph.D. degree in Electrical and Electronics Engineering, specialized in control systems, from the University of Manchester, in 2007. He is currently a senior lecturer in dynamics modelling and control in Queen Mary University of London, UK. His current research interests include constrained optimal control, model predictive control, adaptive robust control and control applications including renewable energies and energy storage, etc.